

## Two-Dimensional, Shell-Cross-linked Nanoparticle Arrays

Qinggao Ma, Edward E. Remsen, Tomasz Kowalewski,<sup>‡</sup> and Karen L. Wooley\*

Washington University, Department of Chemistry  
One Brookings Drive, St. Louis, Missouri 63130-4899

Received February 9, 2001

Revised Manuscript Received March 28, 2001

Ordered arrays of shell-cross-linked (SCK) nanoparticles are formed at substrate surfaces through the precise manipulation of charged groups in the SCK shell. The shell cross-linking chemistry adjusts the particle surface charge and structural rigidity to control the interparticle spacing and particle shape when assembled on a substrate. With the establishment of synthetic methodologies for preparing well-defined nanostructured materials,<sup>1</sup> the development of techniques to manipulate and assemble nanoscale components into a new generation of functional, addressable superstructured materials is the new frontier challenging the advancement of this field.<sup>2</sup> Nanomaterial assembly into two-dimensional (2-D) arrays represents a first step toward the construction of designed superstructured materials. The technological importance of 2-D nanoscale assembly has been widely recognized as evidenced by the development of 2-D colloidal arrays<sup>3</sup> for use as coatings,<sup>4</sup> chemical sensors,<sup>5</sup> and photonic crystals.<sup>6</sup> Until recently, emulsion polymerized latex particles typically have been employed in 2-D colloidal array assembly<sup>7</sup> because they exhibit narrow particle size distributions and strong interparticle interactions. Polymer micelles are a class of technologically important supramolecular materials of well-defined nanoscale dimension that possess an amphiphilic, core-shell morphology. Möller and co-workers<sup>8</sup> used block copolymers of polystyrene and poly(2-vinylpyridine) to form inverse micelles that ordered noble metals into nanoparticle arrays on mica surfaces. The general applicability of polymer micelles is, however, limited by their dynamic structure. In this communication, we report the formation of ordered arrays resulting from robust SCKs. The inherent chemical control of

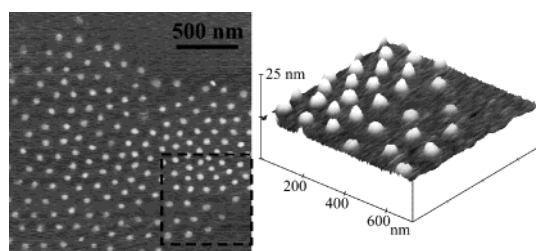
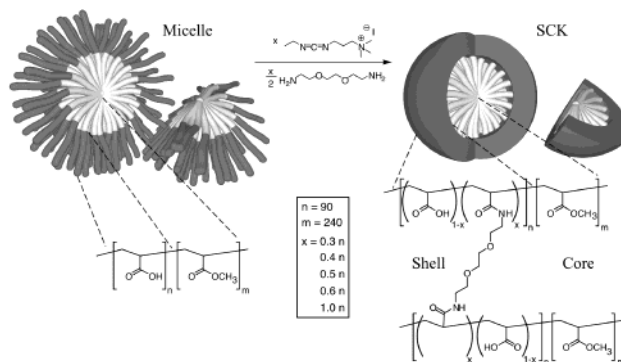


**Figure 1.** Tapping-mode AFM height image of the SCKs prepared with  $x = 0.4n$  (see Scheme 1), deposited ( $1 \mu\text{L}$ ) from aqueous solution ( $5 \mu\text{g/mL}$ ) onto freshly cleaved mica and allowed to dry freely in air for 30 min. The inset shows the three-dimensional rendering of an expanded region of the image area to illustrate the height and interparticle spacing differences for particles located along the outermost array edge and proceeding inward.

### Scheme 1



SCK shell composition needed to manipulate nano-array formation is demonstrated.

Preparation of the SCKs employed a previously described procedure<sup>9</sup> (Scheme 1), which produced SCKs containing acrylicamide-based cross-links. The stoichiometry of the amine-to-acid functionalities controlled the extent of cross-linking and the proportion of remaining carboxylates.

SCKs derived from a PAA<sub>90</sub>-*b*-PMA<sub>240</sub> block copolymer having 40% conversion of the acrylic acid groups were nearly monodisperse in size and had a number-average hydrodynamic diameter ( $D_n$ ) of  $48 \pm 2$  nm in water (Nanopure 18 M $\Omega$ /cm), as measured by dynamic light scattering (DLS). Atomic force microscopy (AFM) characterization of the SCKs deposited onto a mica substrate from this aqueous dispersion yielded images of particles with a number-average height of  $6.2 \pm 2.2$  nm and diameter of  $51.2 \pm 5.8$  nm, without compensation for AFM tip effects. Transmission electron microscopy (TEM) imaging, obtained for a sample deposited onto a carbon-coated copper grid, gave a number-average diameter of  $30.3 \pm 2.6$  nm. The structural model for the SCK supported by DLS, AFM, and TEM data is a swollen nanoparticle (due to the hydrogel-like shell layer) of maximum diameter in aqueous solution, and a flattened nanoparticle (due to the low  $T_g$  (11 °C) PMA core) when deposited and dried onto solid substrates.

The most striking feature of the AFM images was the formation of surface-segregated nano-arrays of the SCKs (Figure 1). Nano-array formation was observed even when the surface density of nanoparticles was insufficient to form uniform monolayers extending over micron length scales. The spacing between particle centers greatly exceeded particle diameters, reminiscent of

(9) (a) Huang, H.; Kowalewski, T.; Remsen, E. E.; Gertzmann, R.; Wooley, K. L. *J. Am. Chem. Soc.* **1997**, *119*, 11653. (b) Ma, Q.; Wooley, K. L. *J. Polym. Sci., Part A: Polym. Chem.* **2000**, *38*, 4805.

\* Corresponding author (klwooley@artsci.wustl.edu).  
<sup>‡</sup> Current address: Carnegie Mellon University, Department of Chemistry, 4400 Fifth Avenue, Pittsburgh, PA 15213.  
 (1) (a) Percec, V.; Ahn, C.-H.; Bera, T. K.; Ungar, G.; Yeardley, D. J. P. *Chem. Eur. J.* **1999**, *5*, 1070. (b) Thurmond, K. B., II; Kowalewski, T.; Wooley, K. L. *J. Am. Chem. Soc.* **1996**, *118*, 7239. (c) Büttin, V.; Billingham, N. C.; Armes, S. P. *J. Am. Chem. Soc.* **1998**, *120*, 12135. (d) Huang, H.; Remsen, E. E.; Kowalewski, T.; Wooley, K. L. *J. Am. Chem. Soc.* **1999**, *121*, 3805. (e) Stewart, S.; Liu, G. *Chem. Mater.* **1999**, *11*, 1048. (f) Sanji, T.; Nakatsuka, Y.; Ohnishi, S.; Sakurai, H. *Macromolecules* **2000**, *33*, 8524. (g) Johnson, S. A.; Ollivier, J.; Mallouk, T. E. *Science* **1999**, *283*, 963.  
 (2) (a) Matijevic, E. *Langmuir* **1994**, *10*, 8. (b) Stupp, S. I.; Pralle, M. U.; Tew, G. N.; Li, L.; Sayar, M.; Zubarev, E. R. *MRS Bull.* **2000**, *25* (4), 42. (c) Hawker, C. J.; Hedrick, J. L.; Miller, R. D.; Volksen, W. *MRS Bull.* **2000**, *25* (4), 54. (d) Taton, T. A.; Mucic, R. C.; Mirkin, C. A.; Letsinger, R. L. *J. Am. Chem. Soc.* **2000**, *122*, 6305. (e) Rueckes, T.; Kim, K.; Joselevich, E.; Tseng, G. Y.; Chenung, C.-L.; Lieber, C. M. *Science* **2000**, *289*, 94.  
 (3) (a) Förster, S.; Antonietti, M. *Adv. Mater.* **1998**, *10*, 195. (b) Kiely, C. J.; Fink, J.; Brust, M.; Bethell, D.; Schiffrin, D. J. *Nature* **1998**, *396*, 444. (c) Shenton, W.; Pum, D.; Sleytr, U. B.; Mann, S. *Nature* **1997**, *389*, 585.  
 (4) Smits, C.; Van Duijneveldt, J. S.; Dhont, J. K. G.; Lekkerkerker, H. N. W.; Briels, W. J. *Phase Transitions* **1990**, *21*, 157.  
 (5) Lee, K.; Asher, S. A. *J. Am. Chem. Soc.* **2000**, *122*, 9534.  
 (6) (a) Rogach, A.; Susha, A.; Caruso, F.; Sukhorukov, G.; Kornowski, A.; Kershaw, S.; Mohwald, H.; Eychmüller, A.; Weller, H. *Adv. Mater.* **2000**, *12*, 333. (b) Mayers, B. T.; Gates, B.; Xia, Y. *Adv. Mater.* **2000**, *12*, 1629. (c) Reese, C. E.; Guerrero, C. D.; Weissman, J. M.; Lee, K.; Asher, S. A. *J. Colloid Interface Sci.* **2000**, *232*, 76.  
 (7) (a) Tandon, S.; Kesavamoorthy, R.; Asher, S. A. *J. Chem. Phys.* **1998**, *109*, 6490. (b) Picard, G. *Langmuir* **1997**, *13*, 3226. (c) Du, H.; Bai, Y. B.; Hui, Z.; Li, L. S.; Chen, Y. M.; Tang, X. Y.; Li, T. J. *Langmuir* **1997**, *13*, 2538.  
 (8) Spatz, J. P.; Mössmer, S.; Hartmann, C.; Möller, M.; Herzog, T.; Krieger, M.; Boyen, H.-G.; Ziemann, P.; Kabius, B. *Langmuir* **2000**, *16*, 407.

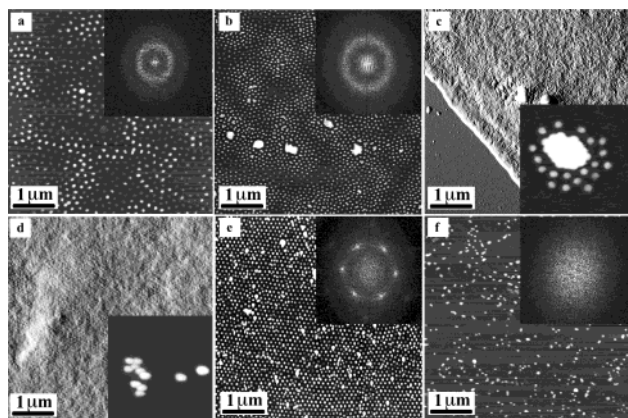


**Figure 2.** Tapping-mode AFM height (a, b, e, f) and amplitude (c, d) images of SCKs, having different degrees of shell cross-linking deposited from aqueous solutions ( $1 \mu\text{L}$ ,  $0.5 \text{ mg/mL}$ ) onto freshly cleaved mica substrates. The SCKs were prepared with degrees of conversion of the carboxylic acid groups to amides ranging from 30% to 100% (theoretical), by controlling the stoichiometries of amine-to-acid (see Scheme 1): (a)  $x = 0.3n$ ,  $H_{\text{av}} = 6.5 \pm 4.4 \text{ nm}$ , interparticle spacing =  $140 \pm 20 \text{ nm}$ ; (b)  $x = 0.4n$ ,  $H_{\text{av}} = 6.2 \pm 2.2 \text{ nm}$ , interparticle spacing =  $110 \pm 20 \text{ nm}$ ; (c)  $x = 0.5n$ ,  $H_{\text{av}} = 7.4 \pm 3.2 \text{ nm}$ ; (d)  $x = 0.6n$ ,  $H_{\text{av}} = 9.9 \pm 3.7 \text{ nm}$ ; (e)  $x = 0.4n$ , with AFM image acquired after centrifugation at 2000 rpm for 10 min, sampling from the center of the centrifuge tube, and deposition onto mica,  $H_{\text{av}} = 5.7 \pm 2.3 \text{ nm}$ ; interparticle spacing =  $100 \pm 10 \text{ nm}$ ; (f)  $x = 0.4n$ , deposited onto AP-mica,  $H_{\text{av}} = 9.2 \pm 3.1 \text{ nm}$ . The insets of a, b, e, and f contain the 2-D Fourier transform power spectra of the corresponding images. The insets of c and d are  $1 \mu\text{m}^2$  images from samples prepared by deposition of  $0.01 \text{ mg/mL}$  SCK solutions.

colloidal crystals forming under the influence of long-range repulsive forces. The AFM image in Figure 1 depicts a sample of SCKs prepared with theoretically 40% conversion of the carboxylic acid groups during cross-linking. This island of arrayed nanoparticles gives a calculated mean nearest-neighbor spacing of  $120 \pm 30 \text{ nm}$ . However, it is clear from the three-dimensional image of the Figure 1 inset that particles near the center of the array are of greater height and shorter interparticle spacings; the particle heights decrease and the interparticle spacings increase on progressing outward toward the edge of the array. We hypothesize that the spacing is controlled by interparticle repulsion of deprotonated carboxylic acid groups remaining after shell cross-linking. Larger interparticle distances between the outermost particles would then be indicative of stronger repulsion due to a greater number of carboxylates resulting from a lower degree of cross-linking. The lowered heights for these particles are also consistent with less-cross-linked particles that would undergo more extensive flattening upon adsorption on mica.

The effects of conversion on the two-dimensional surface assembly behavior of the SCKs were then studied by analyses of individual samples prepared with 0.3, 0.4, 0.5, and 0.6 amine-to-acid stoichiometries to achieve theoretical extents of conversion of 30, 40, 50, and 60%, respectively. As shown in Figure 2, a SCK prepared by cross-linking less than or equal to 40% of available acrylic acids in the shell of its polymer micelle precursor produced hexagonal packing of nanoparticles over length scales greater than  $1 \mu\text{m}$ . The mean distances of interparticle spacing in the nano-arrays were  $140 \pm 20$  and  $110 \pm 20 \text{ nm}$  for the SCKs of 30% and 40% conversion, respectively, as determined by the 2-D Fourier transform power spectra generated from the AFM

images. Ordering for SCKs cross-linked at levels greater than 40% was limited to length scales of 100 to 200 nm and significant aggregation was observed. Only at low SCK solution concentrations was nano-array formation observed; the effects of concentration presently are being studied in more detail. The loss of nano-array formation with increasing percent conversion (comparison of Figure 2a–d) suggests a threshold level of electrostatic repulsion is required to balance attractive and repulsive forces that influence surface diffusion. The particle heights increased with increasing extents of cross-linking (Figure 2a–d). The heterogeneity observed in the image of Figure 1 is also seen in Figure 2b. However, fractionation by sampling following centrifugation resulted in a more homogeneous particle size that exhibited enhanced hexagonal ordering, as noted in the image and corresponding power spectrum of Figure 2e.

The formation of SCK nano-arrays on the negatively charged mica substrate is clearly the product of competing nanoparticle–substrate and nanoparticle–nanoparticle interactions. Previous investigators have cited particle–particle and particle–substrate electrostatic interactions,<sup>7</sup> van der Waals forces,<sup>10</sup> hydrophobic interactions,<sup>11</sup> and capillary forces<sup>12</sup> as driving particle array formation. The influence of surface–nanoparticle interactions on nano-array formation was characterized by comparing AFM images of SCKs deposited on mica with AFM images obtained using positively charged AP-mica.<sup>13</sup> The 40% cross-linked SCK exhibited a random surface distribution of nanoparticles on AP-mica (Figure 2f). The stark contrast between mica and AP-mica as substrates for ordering SCKs into nano-arrays highlights the delicate balance of forces leading to SCK nano-array formation.

The influence of electrostatic interactions on SCK nano-array formation was further investigated by evaluating the net charge on the SCKs via  $\zeta$ -potential measurements by electrophoretic light scattering (ELS). The  $\zeta$ -potential was negative when the SCK nanoparticles were dispersed in pH 8.0, 0.1 M tris-HCl buffer. As the carboxylate conversion for the SCKs increased from 30, 40, 50, and 60%, less negative  $\zeta$ -potentials ( $-45 \pm 2$ ,  $-32 \pm 1$ ,  $-23 \pm 2$ , and  $-6 \pm 2 \text{ mV}$ , respectively) resulted. The trend in  $\zeta$ -potential reflects a progressive loss of net negative charge on the SCK due to the formation of neutral amide groups.

The SCKs serve as a nanoscale component of highly tunable size and net charge: two factors that are key to the formation of well-defined two-dimensional arrays with long-range order. The demonstration of SCK nanoparticles as chemically controllable building blocks for nano-arrays suggests a broader role for these materials in functional superstructure assembly. Further studies to establish the mechanistic details of SCK nano-array formation, including the pH and electrolyte concentration dependence, are in progress.

**Acknowledgment.** The use of a Beckman Coulter Company ELS instrument to measure  $\zeta$ -potentials is appreciated. We also thank Christopher G. Clark, Jr., for generating nanostructure illustrations, and G. Michael Veith for TEM imaging. Funding of this research by the National Science Foundation (DMR-9974457) is gratefully acknowledged.

JA0156542

(10) Grant, M. L.; Saville, D. A. *J. Phys. Chem.* **1994**, *98*, 10358.

(11) Patil, V.; Sastry, M. *Langmuir* **1998**, *14*, 2707.

(12) Denkov, N.; Velev, O.; Kralchevski, P.; Ivanov, I.; Yoshimura, H.; Nagayama, K. *Langmuir* **1992**, *8*, 3183.

(13) The AP-mica surface was formed by treatment of the freshly cleaved mica with 3-(aminopropyl)triethoxysilane (APTES) as per: Shlyakhtenko, L. S.; Gall, A. A.; Weimer, J. J.; Hawin, D. D.; Lyubchenko, Y. L. *Biophys. J.* **1999**, *77*, 568.